

# A Study on Modal Characteristic of Elevated Bridge in Different Construction Stage

Ping Yu CHEN<sup>1</sup>, Kahori IYAMA<sup>2</sup>, Hitoshi MORIKAWA<sup>2</sup>, Kimitoshi SAKAI<sup>3</sup>, and Hikaru KITAMURA<sup>4</sup>

<sup>1</sup>Student Member of JSCE, Tokyo Institute of Technology  
(4259, Nagatsutacho, Midori Ward, Yokohama, Kanagawa 226-8503, Japan)  
E-mail: [chen.p.ac@m.titech.ac.jp](mailto:chen.p.ac@m.titech.ac.jp)

<sup>2</sup>Member of JSCE, Tokyo Institute of Technology  
E-mail: [morikawa.h.aa@m.titech.ac.jp](mailto:morikawa.h.aa@m.titech.ac.jp)

<sup>3</sup>Member of JSCE, Railway Technical Research Institute

<sup>4</sup>Japan Railway Construction, Transport and Technology Agency

The frequency domain decomposition (FDD) technique is convenient to identify the modal characteristics of structures. The FDD technique assumes that the input motion is white noise. The applicability of FDD technique is analytically extended to apply on impact responses which is impulse function of input motion, and it is confirmed by using observed data. Furthermore, the FDD technique is applied to an elevated bridge at different construction stages. Modal characteristics of the elevated bridge are identified and discussed.

**Key Words :** modal identification, Frequency Domain Decomposition, microtremor, impact test, elevated bridge

## 1. INTRODUCTION

Under the current design code of elevated bridge for railroad, single span bridges are considered individually. During the construction of elevated bridge, when two single span bridges were connected with a superstructure, modal characteristic would change obviously<sup>1</sup>. It is important to understand the changes of modal characteristic on different construction stages especially during earthquake-resistant design. Therefore, different elevated bridge in each construction stage was analyzed and compared along with the construction process.

Modal identification of output-only system is now widely used in civil engineering to understand the dynamic behavior of structures, especially during earthquake resistant design. Frequency Domain Decomposition (FDD) technique is a user-friendly and high accuracy technique applied to output-only system, and assumed input as white noise<sup>2</sup>. Therefore, microtremor which is a low amplitude ambient vibration was analyzed by using FDD technique to obtain modal parameters in this study.

Modal identification by using impact test is often associated with input and output system. The applicability of FDD technique applied to impact test is

shown by comparing the expanded equation between input characteristic and modal characteristic<sup>3</sup>.

Furthermore, the FDD technique is applied to the simultaneous multipoint observation records of microtremor and impact test for single and continuous span bridges in this study. Modal characteristics are identified and discussed at different construction stages.

## 2. APPLICABILITY OF FDD TECHNIQUE APPLIED TO IMPACT TEST

The output power and cross spectrum matrix can be expressed as:

$$G_{yy} \approx \sum_{k=1}^N \sum_{s=1}^N \{ [B_{ks}] + [\bar{B}_{ks}]^T \} \quad (1)$$

where

$$[B_{ks}] = \frac{c_{sk}/\bar{d}_s d_k}{\{\sigma_k + j(\omega - \omega_{dk})\}(\sigma_{ks} - j\Delta\omega_{dks})} \{ \bar{\varphi}_s^y \} \{ \varphi_k^y \}^T, \\ \sigma_{ks} = \sigma_k + \sigma_s, \quad \Delta\omega_{dks} = \omega_{dk} - \omega_{ds}, \\ d_k = 2jm_k \omega_{dk}, \quad c_{sk} = \{ \bar{\varphi}_s \}^T [G_{XX}] \{ \varphi_k \} \quad (2)$$

here  $k, s$  are mode number,  $\omega_d$  is damped circular

frequency,  $\sigma$  is modal damping ratio,  $\{\varphi\}$  is modal vector.  $\{\varphi^y\}$  is the modal vector of observation point.

From eq.(2),  $c_{sk}$  shows the input characteristic of a system. If a vibration system is assumed as proportional damping system which modal vector is in real number,  $c_{sk}$  can be rewritten as:

$$c_{sk} = \sum_{l=1}^N \sum_{m=1}^N \bar{\varphi}_{sl} \varphi_{km} \langle \bar{X}_l \cdot X_k \rangle \quad (3)$$

where  $\langle \cdot \rangle$  shows ensemble average of  $\bar{X}_l, X_k$ . What's more, in ideal microtremor input system or impulse input equal to 1, there is no relationship between each input in each observation point

$$\langle \bar{X}_l \cdot X_k \rangle = \begin{cases} X_{lk} & (l = k) \\ 0 & (l \neq k) \end{cases}$$

Thus, if the assumption of  $X_{lk} \cong X_a$  (constant) is valid, when the observation point 'I' is excited by an impulse which amplitude is much bigger than microtremor  $X_I (\gg X_a)$ , eq.(3.) can be derived as:

$$c_{sk} = \begin{cases} X_a \sum_{l=1}^N \varphi_{sl} \varphi_{kl} & (\text{microtremor}) \\ X_a \sum_{l=1}^N \varphi_{sl} \varphi_{kl} + X_I \varphi_{sl} \varphi_{kl} & (\text{impact}) \end{cases} \quad (4)$$

Furthermore, mode orthogonality is applied to eq.(4.):

$$c_{sk} = 0, c_{kk} = \begin{cases} \bar{X}_a & (\text{microtremor}) \\ \bar{X}_a + X_I \varphi_{kl}^2 & (\text{impact}) \end{cases} \quad (5)$$

when  $\bar{X}_a$  is a constant, eq(1.) can be derived as:

$$[G_{YY}] \approx \sum_{k=1}^N \{ [B_{kk}] + [\bar{B}_{kk}]^T \}$$

here  $\{ \}$  in right hand side of the equation is expanded and is derived as:

$$[G_{YY}] \approx \sum_{k=1}^N \alpha_k(\omega) \{ \varphi_k^y \} \{ \varphi_k^y \}^T \quad (6)$$

where

$$\alpha_k(\omega) = \frac{1}{4m_k^2 \omega_{dk}^2 \sigma_k^2 + (\omega - \omega_{dk})^2} \quad (7)$$

$\alpha_k(\omega)$  is modal power spectrum with peak when  $\omega = \omega_{dk}$ . In FDD technique, the shape of eq.(6.) is identical to singular value decomposition (SVD). Therefore, the first singular value derived from singular value decomposition applied to  $[G_{YY}]$  is approximate to  $\alpha_1(\omega)$ . Thus, peaks and corresponding natural frequencies in  $\alpha_1(\omega)$  can be identified, and first singular vector which is corresponding to  $\{ \varphi_1^y \}$  can be identified as modal shape as well.

Same mode that can be identified in both microtremor and impact test is demonstrated previously in eq(5.) and eq(7.). However, this mode may become a dominant mode and other modes may not be able to be seen in impact test because  $\alpha_k(\omega)$  is extremely enlarged by impulse at the dominant mode.

### 3. FIELD OBSERVATION AND ANALYSIS

#### (1) Setting of observations

The field observation was carried out at an under-construction elevated railroad bridge, and five-time observations were performed at different construction stages. Fig.1 shows the schematic figure of whole the target bridge after construction was completed. Observation cases are listed in Table 1: two cases for single span bridge (2015/12 and 2017/11) and three cases for continuous span bridge (2016/10, 2019/01, and 2019/07). Here, Ct\* were superstructure supported with rubber support on both ends of adjacent rigid-frame structures R\*. In whole the observations, microtremors were observed, furthermore, impact tests were performed in the case of 2015/12, 2016/10, and 2017/11.

Two velocity sensors KVS300 and CR4.5, and one accelerometer Titan, and four types of data loggers, Geodas, OTK, AK, LS8800, and LS7000XT were used in each observation. Fig.2 shows the sensor collocations and also positions and directions of the impacts for impact tests.

#### (2) Analysis

The observed microtremor records were divided by portions of 40.96 second length. For impact test data, a free-decay portion of 40.96 second length was selected from each impact response. The fast Fourier transform (FFT) was applied to each portion.

Next, power and cross spectra were calculated from each portion by FFT and they were averaged over the portions. Singular values and singular vectors were calculated by applying SVD to  $[G_{YY}]$ , which consisted of power and cross spectra. Dominant peaks in 1<sup>st</sup> singular value spectrum were picked up and they were identified as eigen frequencies, which are called peak frequencies, hereafter. The corresponding singular vectors were selected as modal vectors.

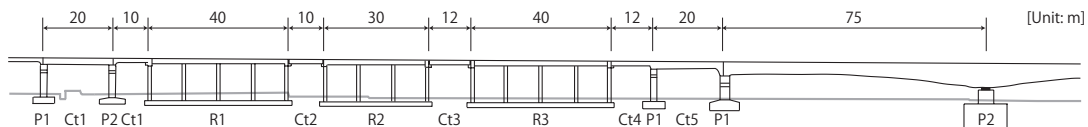
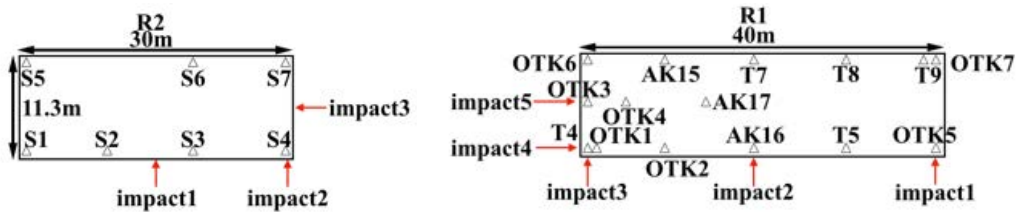


Fig.1 Profile of the elevated bridge.

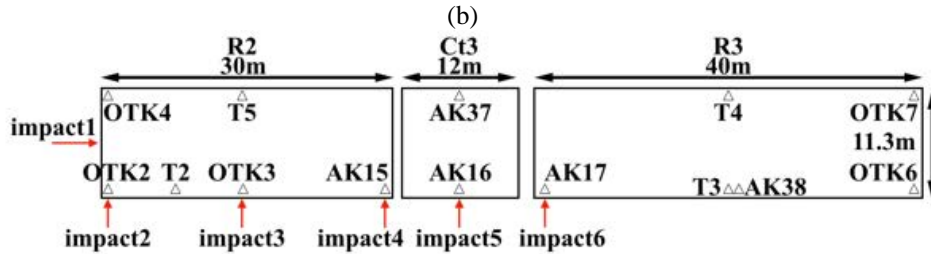
**Table 1** Observed cases

Cases	Region	Sensor	Logger	Sampling Rate (Hz)	Microtremor duration (min)	Impact test repeats (times)
2015/12	R2	CR4.5	Geodas	200	20	10
2016/10	R2~R3	KVS	OTK	200	20	10
		KVS	AK	100		
		Titan	LS8800	200		
		Titan	LS7000XT	200		
2017/11	R1	KVS	OTK	200	45	14
		KVS	AK	100		
		Titan	LS8800	200		
2019/01	Ct1~Ct4	KVS	OTK	200	60	
		KVS	AK	100		
		Titan	LS8800	200		
		KVS	LS7000XT	200		
2019/07	Ct1~Ct5	KVS	OTK	200	60	
		KVS	AK	100		
		Titan	LS8800	200		

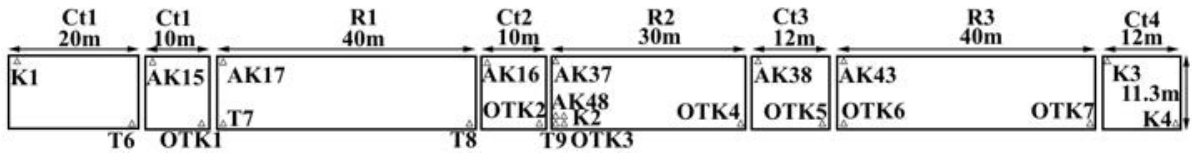


(a) 2015/12

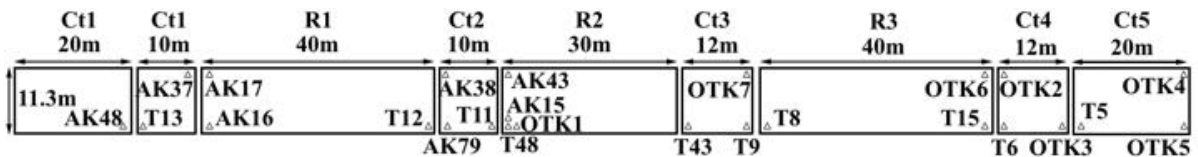
(c) 2017/11



(b) 2016/10



(d) 2019/01



(e) 2019/07

**Fig.2** Sensors collocation and positions and directions of impacts

## 4. RESULTS AND DISCUSSIONS

### (1) Applicability of applying FDD to impact test

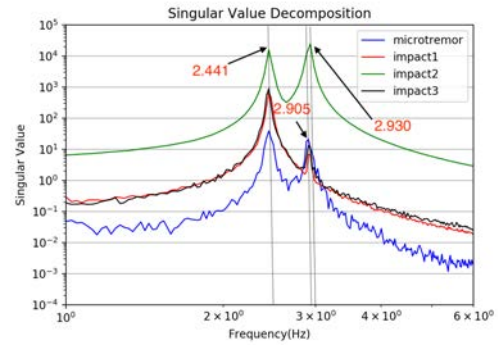
Fig.3 shows 1<sup>st</sup> singular values of microtremors and impact responses for case 2015/12. Two peaks are recognized for all data, even though the magnitude of dominant mode in the singular value is different obviously. The peak frequencies and corresponding modal shapes are shown in Table 2. The modal shapes at 1<sup>st</sup> and 2<sup>nd</sup> peak frequencies, 2.441 Hz and 2.905 Hz, respectively, are similar shapes, however, modal shape of impact 2 predominates transversal direction, and microtremor and impact 1 and 3 predominate longitudinal direction at the 1<sup>st</sup> peak frequency. This difference of modal shape at 1<sup>st</sup> peak frequency suggests that two different modes are overlapped at the same frequency of 2.441 Hz: translational modes with transversal and longitudinal directions. According to its design calculation, the eigen frequencies are very close for the translational modes of transversal and longitudinal directions, which are 1.96 and 2.02 Hz, respectively. Furthermore, the shape of 2<sup>nd</sup> singular value spectrum is similar to 1<sup>st</sup> one around frequency 2.441 Hz as shown in Fig.4. The singular vector corresponding to 2<sup>nd</sup> singular value at frequency 2.441 Hz predominates the translational mode with transversal direction. These results support the above suggestion. It is observed that only the impact 2 shows large value of singular value around the second peak frequency, 2.930 Hz. This means that the position of the impact of impact 2 can excite the rotational mode effectively.

**Table 2** Modal shape of case 2015/12.

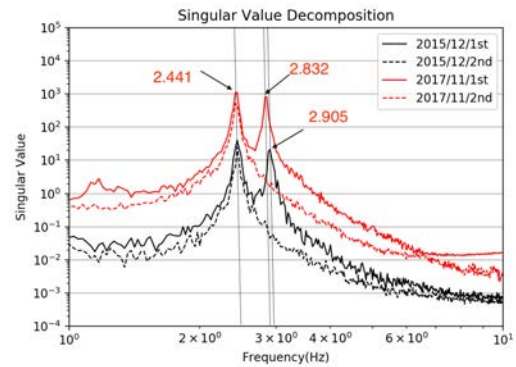
	Microtremor	Impact test		
		Case 1	Case 2	Case 3
Frequency	2.441 Hz	2.441 Hz	2.441 Hz	2.441 Hz
Modal shape (1 <sup>st</sup> singular value)				
Frequency	2.905 Hz	2.905 Hz	2.930 Hz	2.905 Hz
Modal shape (1 <sup>st</sup> singular value)				

Table 3 and Fig.4 shows the summary of peak frequencies and modal shapes for case 2017/11 and 1<sup>st</sup> and 2<sup>nd</sup> singular value spectra, respectively. These figures show similar properties to those of case 2015/12. Thus, generally speaking, it is suggested

that (1) two translational modes and rotational mode are excited for a single span bridge, and (2) these modes can be identified using both microtremor and impulse response.



**Fig.3** 1<sup>st</sup> singular value spectrum in case 2015/12.



**Fig.4** 1<sup>st</sup> and 2<sup>nd</sup> singular value of case 2015/12 and 2017/11 for microtremor.

**Table 3** Modal shape of case 2017/11.

Mode	real	abs
Cases/ Peaks	Peak 1	Peak 2
Microtremor	2.441	2.832
Impact1	2.441	2.832
Impact2	2.441	2.832
Impact3	2.441	2.832
Impact4	2.441	2.832
Impact5	2.441	2.832

Fig.5 shows the singular value spectra in case 2016/10 and the peak frequencies and corresponding modal shapes are summarized in Table 4. The peak frequencies can be identified at same values for both microtremor and impact responses. However, the predominant peak at frequency 1.879 Hz does not appear in the singular value spectra of microtremor. Impact test can excite modes which do not appear in

microtremor, in a case of complicated structure.

The FDD technique can apply to impact test, and the combination of microtremor and impact test can cover most of possible modes.

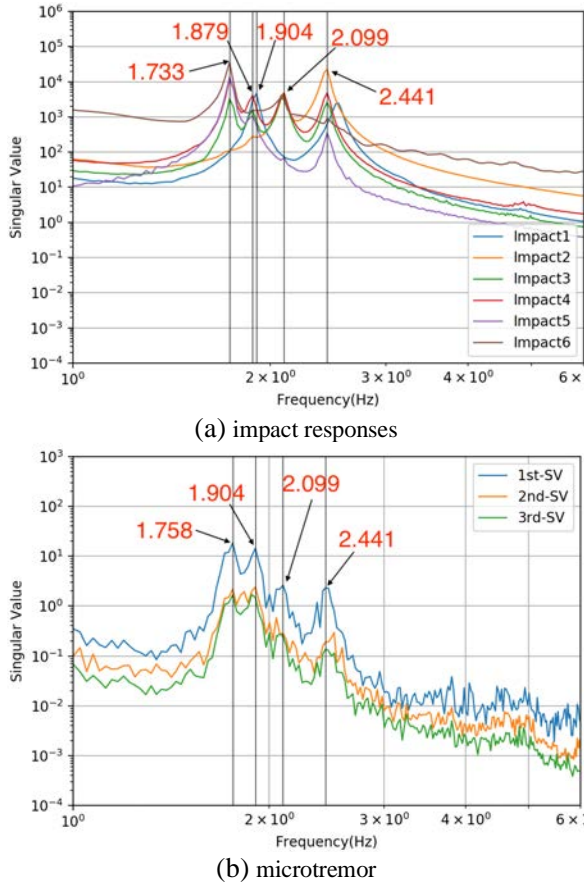


**Fig.5** 1<sup>st</sup> singular value spectra for impact responses and 1<sup>st</sup> to 3<sup>rd</sup> singular value spectra for microtremor.

**Table 4** Modal shape of case 2016/10.

Mode	Modal Shapes				
---real					
---abs					
Cases/ Peaks	Peak 1	Peak 2	Peak 3	Peak 4	Peak 5
Microtremor	1.758	—	1.904	2.099	2.441
Impact1	—	—	1.904	—	—
Impact2	—	—	—	2.099	2.441
Impact3	1.733	1.879	—	2.099	2.441
Impact4	1.733	1.879	—	2.099	2.441
Impact5	1.733	1.879	—	—	2.441
Impact6	1.733	—	—	2.099	2.441

## (2) Modal characteristics at different construction stages

It is observed from Tables 2, 3, and 4 that the 1<sup>st</sup> peak frequency for continuous span bridge is lower

than one of single span bridge. Fig.6 shows the singular value spectra of cases 2019/01 and 2019/07. The difference between these two cases is the existence of Ct5, which connects rigid-frame structures to long-spanned and heavy bridge. Table 5 lists the peak frequencies and modal shapes, which is drawn under an assumption of rigid floor of the superstructure. The modal shape at 1<sup>st</sup> peak frequency for the two cases, 2019/01 and 2019/07, show the similar modal shapes, in which only Ct3 is excited. Furthermore, these modal shapes are identical to the 1<sup>st</sup> mode of case 2016/10, whose peak frequencies are 1.708 to 1.758 Hz. The modal shape at 2<sup>nd</sup> peak frequency for case 2019/07 is similar to the 3<sup>rd</sup> one for case 2019/01, in which only Ct2 is excited. The other modes show no obvious relevant between the two cases. The modal shapes identified from microtremors seem to be formed by adjacent at most three units.

Differences of the modal shapes between two cases of 2019/01 and 2019/07 are affected by an additional superstructure, Ct5. The modal shape at 3<sup>rd</sup> peak frequency for case 2019/07 dominates a translational mode with longitudinal direction. This may be effects of the constraints by the connected structures through Ct5.

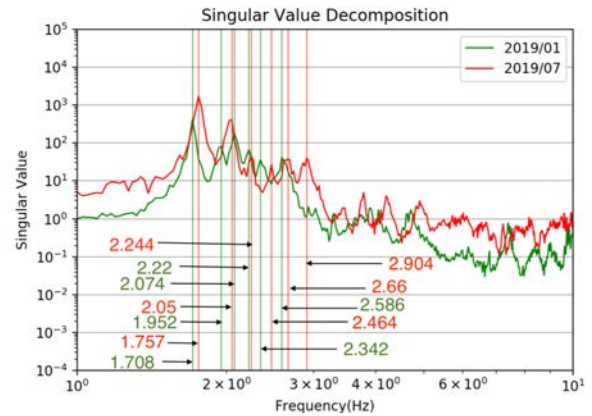


**Fig.6** 1<sup>st</sup> singular value spectra of case 2019/01 and 2019/07.

## 5. CONCLUSION

The applicability of FDD technique applied to impact responses were demonstrated through theoretical analysis and experimental data. Impact test can provide almost same modes with those of microtremor for single span bridge. Furthermore, the impact test can excite hidden modes which are not identified by microtremor.

Modal characteristics at different construction stages were presented for continuous span bridge. The fundamental modal shapes seem to be formed by adjacent at most three units of superstructures. The constraints by connection of superstructures affect the modal shapes obviously.

**Table 5** Modal shape of case 2019/01 and 2019/07.

Cases/Peaks	Microtremor	Mode ( ----real ----abs) 2019/01							
		Ct1	R1	Ct2	R2	Ct3	R4	Ct4	
Peak1	1.708								
Peak2	1.952								
Peak3	2.074								
Peak4	2.22								
Peak5	2.342								
Peak6	2.586								
Cases/Peaks	Microtremor	Mode ( ----real ----abs) 2019/07							
		Ct1	R1	Ct2	R2	Ct3	R4	Ct4	Ct5
Peak1	1.757								
Peak2	2.05								
Peak3	2.244								
Peak4	2.464								
Peak5	2.66								
Peak6	2.904								

**REFERENCES**

- 1) Ping Yu, C. et al. : Modal Identification of Elevated Bridge through Microtremor and Impact test using Frequency Domain Decomposition, *Japan Society of Civil Engineers 2019 Annual Meeting*.
- 2) Brinker, R., Zhang, L., Anderson, P. : Modal Identification of Output-only Systems Using Frequency Domain Decomposition, *Smart Materials and Structures*, 10, pp. 441-445, 2001.
- 3) Morikawa, H. et al.: Applicability of Frequency Domain Decomposition Technique on Structural Modal Identification for Impact test, *Japan Society of Civil Engineers 2019 Annual Meeting*.

(Received September 10, 2019)  
(Accepted ???)